Journal of Superconductivity and Novel Magnetism (2020) 33:1215–1222
https://doi.org/10.1007/s10948-019-05340-0

ORIGINAL PAPER

Half-Metallic Ferromagnetism in Gd-Doped $Ti_{1/2}Mg_{1/2}N$ Alloy: An ab initio Prediction

Z. Haddouche[1] · A. Hallouche[1] · A. Dahani[1,2] · A. Zaoui[1] · S. Kacimi[1] · Y. El Ahmar[1] · A. Kadiri[1] · M. Djebari[1] · A. Boukortt[3]

Received: 5 September 2019 / Accepted: 14 October 2019 / Published online: 23 November 2019
© Springer Science+Business Media, LLC, part of Springer Nature 2019

Abstract
In this work, we have investigated the electronic and magnetic properties of gadolinium Gd-doped $Ti_{0.5}Mg_{0.5}N$ alloy. The supercell of 32 atoms was generated by the Alloy Theoretic Automated Toolkit (ATAT), and then we have used first-principles calculations performed by the full-potential linearized augmented plane wave method based on the spin density functional theory within the generalized gradient approximation of Perdew-Burke-Ernzerhof and the modified Becke-Johnson potential. We have also performed GGA + U calculations describing the strong correlation between the 4f electrons in Gd. Both GGA and mBJ calculations have shown that $Ti_{0.5}Mg_{0.5}N$ alloy depicted a semiconductor character with band gaps of 0.403 eV and 1.184 eV, respectively. The calculated atomic-resolved densities of states of $Ti_6Gd_2Mg_8N_{16}$ alloy predict the half-metallic character (HMs) with ferromagnetic order (FM) using the modified Becke-Johnson potential mBJ. We have also estimated the Curie temperatures by using the Heisenberg model in the mean field approximation.

Keywords L/APW + lo · DFT + U · Magnetic structure · Diluted magnetic semiconductors

1 Introduction

Since the discovery of the half-metallic (HM) ferromagnetism character by Groot et al. in AMnSb (A = Ni, Pt) [1] in 1983, the scientific community has not ceased to dig in this voice for the purpose to find new HM ferromagnets, which are more promising for spintronic devices applications [2]. As it's known for the electronic structure of the half-metallic ferromagnets, the two spin bands show a different character where the majority spin band is metallic and the minority spin band is semiconducting with the gap at the Fermi level leading to 100% carrier spin polarization. The motive behind all these researches is to replace the conventional electronic materials by more new competitive materials where a degree of freedom, offered by the spin, plays an important role allowing a gain of speed in data processing communication and low energy consumption [3]. In the past decade, a lot of many half-metallic ferromagnets have been carried out listed up to now in three main classes [4]: Heusler alloys such as Mn_2VZ (Z = Ga, Ge, Sn, Al, In) [5]; binary systems with zinc blende (ZB) or diamond structures such as MnBi and MnAs [6, 7]; and oxides such as CrO_2 [8] and Fe_3O_4 [9]. However, the majority of these half-metallic ferromagnets mentioned above are based on Mn^{2+} since their physical properties are not complicated. The 3d states are half occupied, and there is no orbital moment (S = 5/2, L = 0) according to Hund's rules. In addition, these states can be inserted without any influence on the crystallographic structure [10]. But for the most of them, the main disadvantage is that they have low Curie temperatures, it is well below room temperature, and rarely do they reach to 100% in spin polarization [11].

To contribute to the quest for new half-metallic ferromagnets and based on the works of Bjorn Alling [12], we present an ab initio study on the doping effect on the electronic and magnetic structure of Gd-doped $Ti_{0.5}Mg_{0.5}N$ alloy.

✉ S. Kacimi
kacimi200x@yahoo.fr

[1] Laboratoire Physique Computationnelle des Matériaux, Université Djillali Liabès de Sidi Bel-Abbès, 22000 Sidi Bel-Abbès, Algeria

[2] Faculty of Technology, University of Saida, Saida, Algeria

[3] Laboratoire d'Elaboration et Caractérisation Physico Mécanique et Métallurgique des Matériaux (ECP3M) Département de Génie Electrique, Faculté des Sciences et de la Technologie, Université Abdel Hamid Ibn Badis de Mostaganem, 27000 Mostaganem, Algeria

The paper is organized as follows: Section II gives a brief description of the method used in the calculations. The calculated results are presented and analyzed in Section III. A summary is presented in Section V.

2 Methodology

The calculations presented here are performed with the code "mcsqs" implemented in the Alloy Theoretic Automated Toolkit (ATAT) [13] to find the structure that best matches the correlation functions of random alloys by leaving from TiN primitive cell with a = 4.24 Å [12]. In this work, we used a special quasirandom structure (SQS) [14] approach to modulate our configurationally disordered alloy TiMgN. We note also that the 32 atoms SQS given in Fig. 1 reproduce the multisite correlation functions of perfectly the fcc alloy. After the determination of the structure and in order to investigate the electronic and magnetic properties of our alloy, we have performed ab initio self-consistent calculations based on the density functional theory (DFT) [15, 16] implemented in the Wien2*k* code developed by Blaha and Peter et al. [17]. The atoms were represented by the full-potential linearized augmented plane wave (FPLAPW) method [18]. In this method, the wave functions, charge densities, and potentials are extended into spherical harmonics without overlapping muffin-tin spheres, and plane waves are used in the remaining interstitial region of the unit cell. In the code, the states of the heart and valence are treated differently. The core states are treated by a relativistic approach of Dirac-Fock, while the valence states are treated by a scalar relativistic approach. The electronic exchange and correlation functions were processed using the generalized gradient approximation of Perdew-Burke-Ernzerhof [19] and the modified Becke-Johnson potential [20], as well as their added versions on the Coulomb interaction, GGA (mBJ) + *U* [21]. The U parameter of the Gd 4*f* orbital varies from 0 to 8 eV. At the same time, we used an appropriate set of *k*-points to calculate the total energy. The bulk modulus and the equilibrium lattice parameter were evaluated using the Murnaghan's state equation [22] to adjust the volume curves as a function of energy. The electronic states of the atoms in the crystal have been chosen with the valence configurations of Ti, $3s^2 3p^6 3d^2 4s^2$; Gd, $4f^7 5d^1 6s^2$; Mg, $3s^2$; and N, $2s^2 2p^3$. The values of 2.2 Bohr for the gadolinium, 1.8 Bohr for titanium, 1.8 Bohr for magnesium, and 1.7 for nitrogen as the muffin-tin (MT) radii were used. The total energy was minimized using a set of 56 *k*-points in the irreducible sector of the Brillouin zone, and the value of 7 for the cutoff energy was used. The self-consistent calculations are considered to be converged only when the calculated total energy of the crystal converged to less than 1 mRy.

The substitutional defects are considered where two Gd ions in the Ti sites were substituted for two possible configurations, near and far as mentioned in Fig. 2.

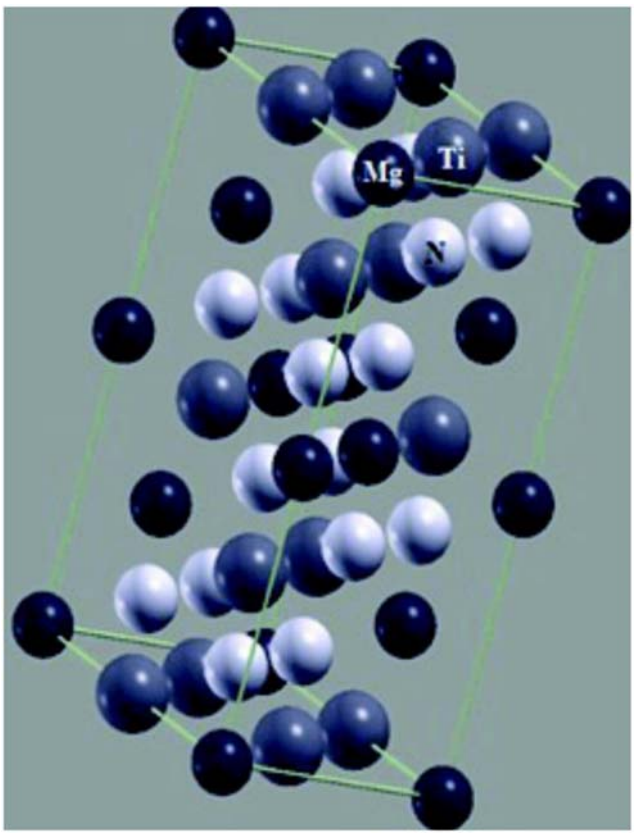

Fig. 1 SQS-32 atoms for x = 0.5 in $Ti_{1-x}Mg_xN$

3 Results and Discussion

3.1 Structural and Electronic Properties of the Alloy Parent

To study the relative stability of $Ti_{0.5}Mg_{0.5}N$ alloy, we have evaluated the formation and cohesion energies. The energy formation is given by the formula:

$$\Delta H = \frac{1}{x+y+z}\left[E_{total} - xE^{A}_{solid} - yE^{B}_{solid} - zE^{C}_{solid}\right] \quad (1)$$

where E_{total} is the total energy of the unit cell and x ,y, and z are the numbers of Ti, Mg, and N atoms, respectively, used in supercell. E^{A}_{solid}, E^{B}_{solid}, and E^{C}_{solid} are the energies per Ti, Mg, and N atoms in the alloy. The calculated energies of Ti, Mg, and N atoms are −1707.28, −400.45, and −109.08 Ry/atom, respectively. The energy formation value is −5.26 eV/atom, which confirm that our alloy is thermodynamically stable.

The cohesive energy also a key factor for determination of stability of crystal, defined as the energy that must be added to

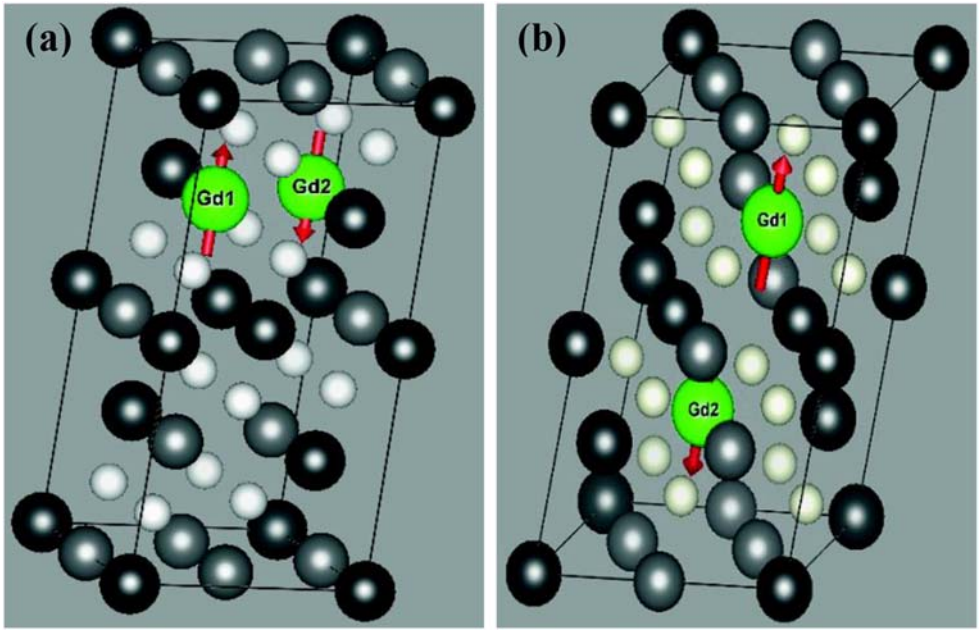

Fig. 2 Near (a) and far (b) positions of Gd ions doped in $Ti_{0.5}Mg_{0.5}N$ alloy

the alloy to separate its components into neutral free atoms, is given by the formula:

$$E_{coh} = \frac{1}{x+y+z}\left[E_{total} - xE^{A}_{atom} - yE^{B}_{atom} - zE^{C}_{atom}\right] \quad (2)$$

where x, y, and z are the numbers of Ti, Mg, and N atoms in unit cell, respectively. E^{A}_{atom},E^{B}_{atom}, and E^{C}_{atom} are the energies of the isolated atoms of Ti, Mg, and N, respectively.

The calculated energies for Ti, Mg, and N isolated atoms are −1707.13, −400.55, and −108.90 Ry/atom, respectively.

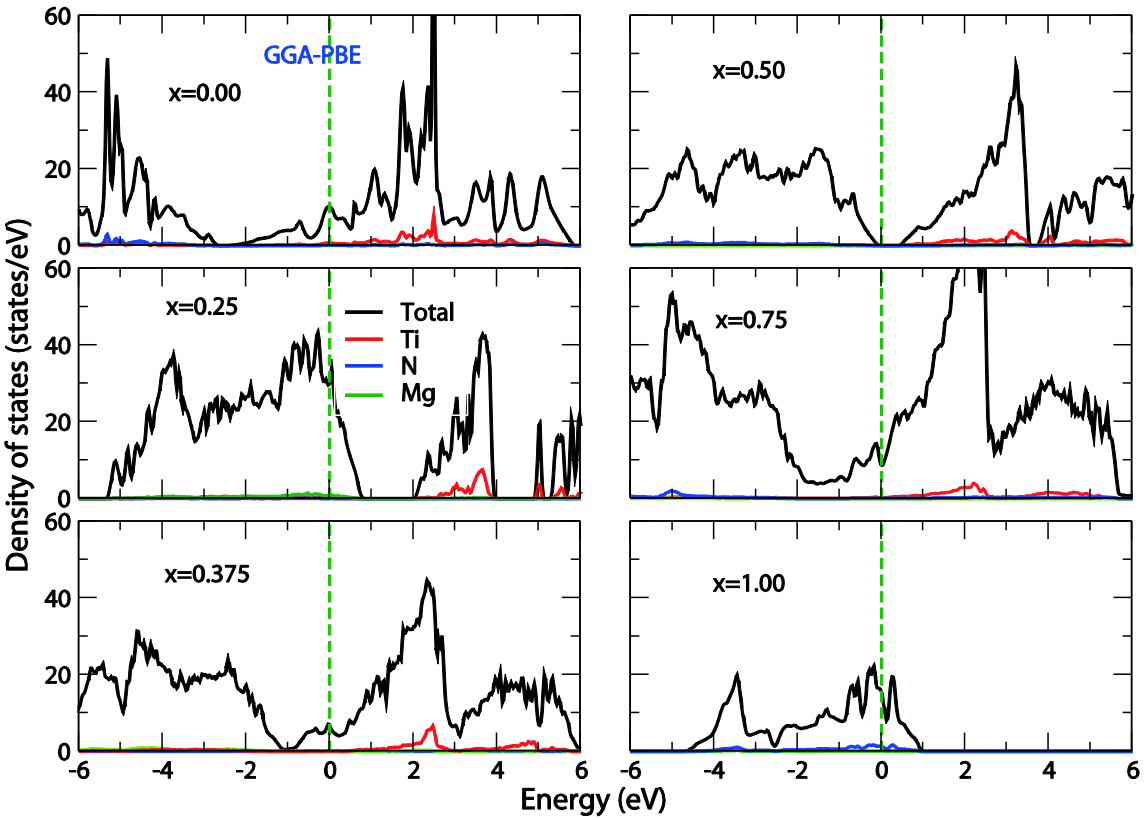

Fig. 3 The total and partial densities of states of $Ti_xMg_{1-x}N$ alloys obtained by the GGA-PBE calculations for $0 \le x \le 1$. The Fermi level is taken at zero energy

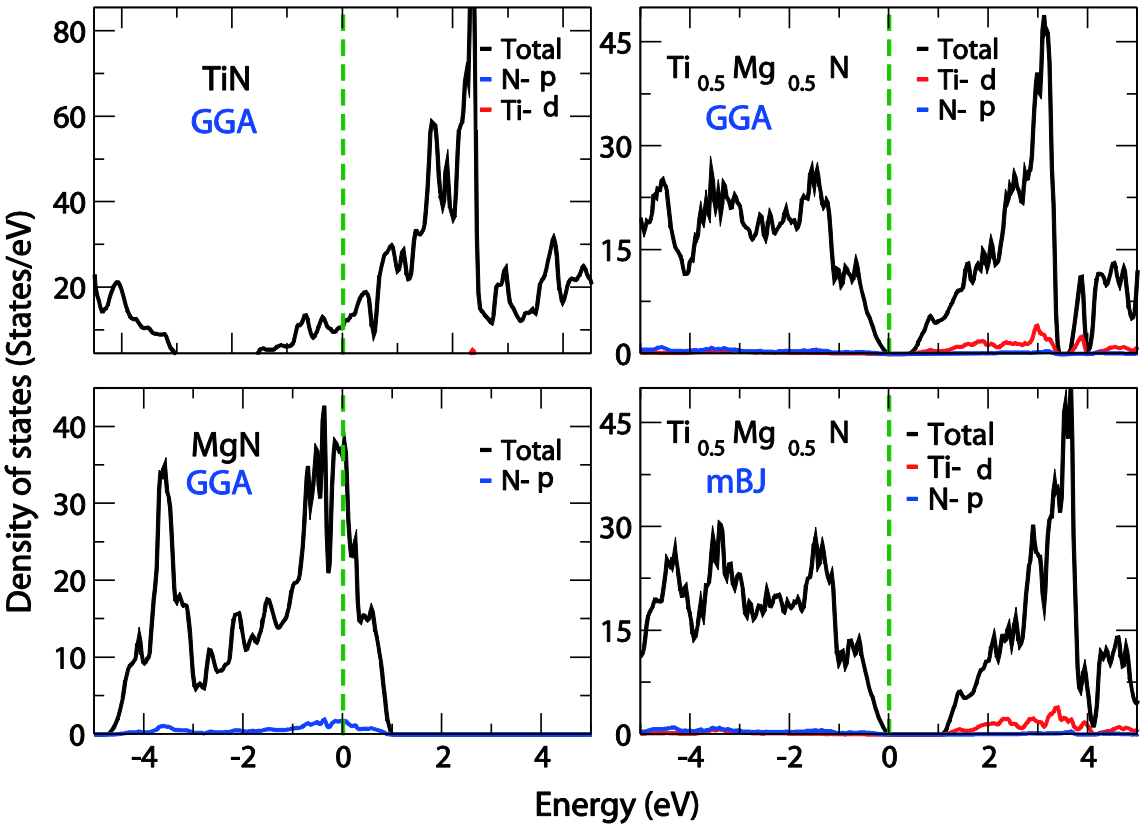

Fig. 4 The total and partial densities of states of TiN, MgN compounds, and their corresponding alloy $Ti_{0.5}Mg_{0.5}N$ obtained by the GGA-PBE and mBJ calculations. The Fermi level is taken at zero energy

So the cohesive energy is −6.65 eV/ atom confirming the stability of this structure.

The total and partial densities of states of pure crystals for TiN, MgN, and their ternary corresponding alloy $Ti_{0.5}Mg_{0.5}N$ are show in Fig. 3. It can be observed that there is no band gap at the Fermi level E_F and hence both crystals TiN and MgN are metallic. For TiN compound near the Fermi level, the DOS is mainly contributed by Ti-*d* states, and the lowest valence band is dominantly by N-*p* states. But for MgN compound, the DOS in the vicinity of E_F is originated from N-*p* orbitals and the bottom of the valence band from Mg-*p* states.

For x = 0.5, $Ti_{0.5}Mg_{0.5}N$ alloy exhibits a semiconductor character.

Recently, the semi-local Becke-Johnson (BJ) exchange-correlation potential and its modified form proposed by Tran and Blaha (TB-mBJ) have attracted a lot of interest because of the remarkable correction reported on the gaps of bands for semiconductors and insulators. In this work, we have also investigated the performance of the TB-mBJ potential for

Table 1 Total energies of $Ti_6Gd_2Mg_8N_{16}$ alloy before and after relaxed atomic internal positions as function of the Hubbard potential

U(eV)	Stability	$E_{unrelaxed}$	$E_{relaxed}$
0	AFM	−60327.7224	−60328.3784
2	FM	−60327.6269	−60328.3404
4	FM	−60327.5335	−60328.3061
6	FM	−60327.4526	−60328.2717
8	FM	−60327.3805	−60328.2439

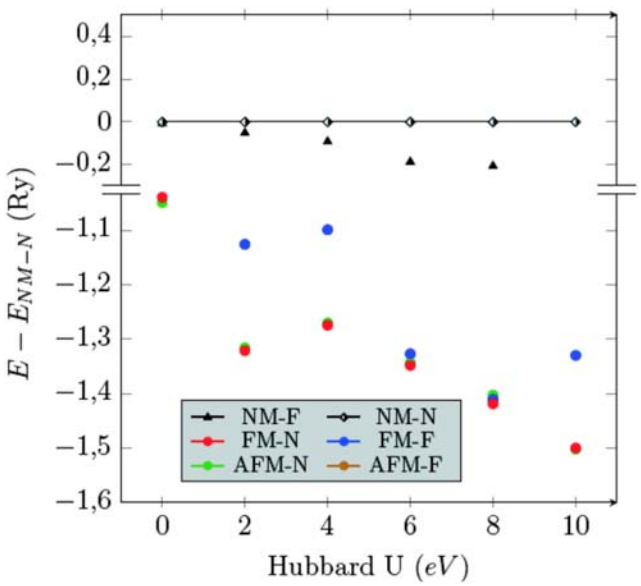

Fig. 5 Magnetic phase stability as a function of the effective Coulomb interaction of $Ti_6Gd_2Mg_8N_{16}$ using GGA + *U* approach

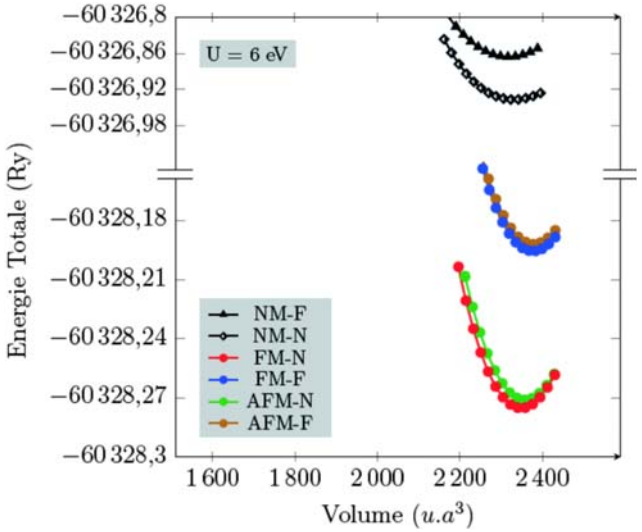

Fig. 6 Calculated total energy versus volume for $Ti_6Gd_2Mg_8N_{16}$ using GGA + *6 eV* approach for different magnetic configurations

the description of electronic structure in $Ti_{0.5}Mg_{0.5}N$ semiconductor.

For more reliable predictions of the band gap energies, the TB-mBJ approximation was used to improve this property (see Fig. 4). The calculated band gaps of $Ti_{0.5}Mg_{0.5}N$ alloy using both GGA and TB-mBJ approximations are 0.403 eV and 1.183 eV, respectively. We conclude that a metal-semiconductor transition is observed when the Mg content is equal to x = 0.5 in $Ti_{1-x}Mg_xN$ alloy. Bjorn Alling [12] predicts a band gap value of 1.3 eV, which is in close agreement with our result. We point out that the use of the TB-mBJ potential gives better results comparing with the GGA approach. Very recently, B. Wang and D. Gall [23] have experimentally validating that $Ti_{0.5}Mg_{0.5}N$ is a semiconductor.

3.2 Gadolinium Doping

In this study, our main purpose is to verify if this alloy can become a diluted magnetic semiconductor via a doping way. For that, a pair of Gd atoms is substituted in Ti near sites at (0.75, 0.625, 0.75) and (0.25, 0.375, 0.75) and in Ti far sites at (0.25, 0.375, 0.75) and (0.75, 0.625, 0.25) for the three different magnetic configurations: ferromagnetic (FM), antiferromagnetic (AFM), and nonmagnetic (NM). We used a generalized gradient approximation (GGA) with the additional Hubbard correction term *U* (GGA + *U*) to describe the strong

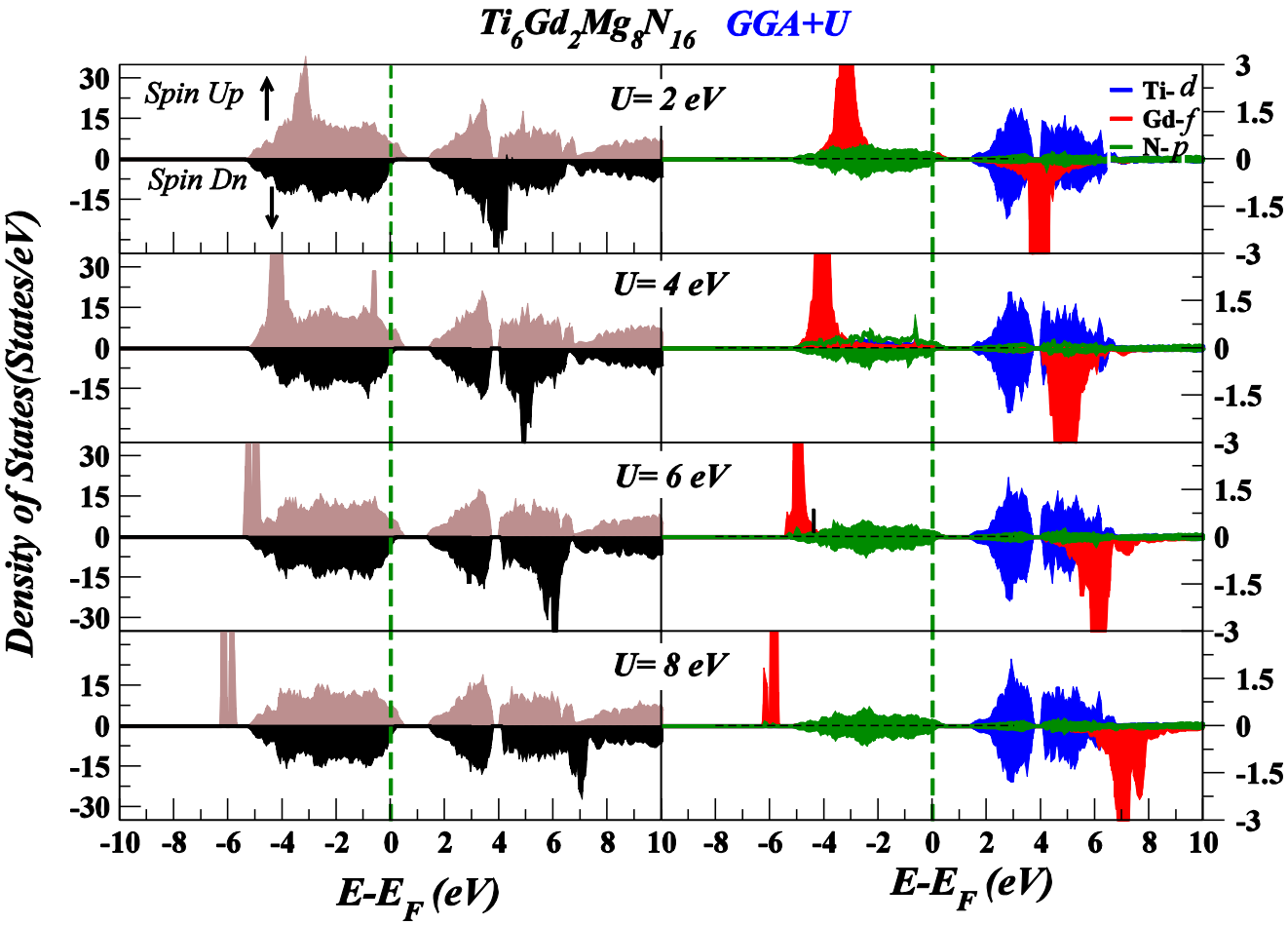

Fig. 7 Total and partial densities of states of the ferromagnetic $Ti_6Gd_2Mg_8N_{16}$ system using GGA + U approach (U varies from 2 eV to 8 eV)

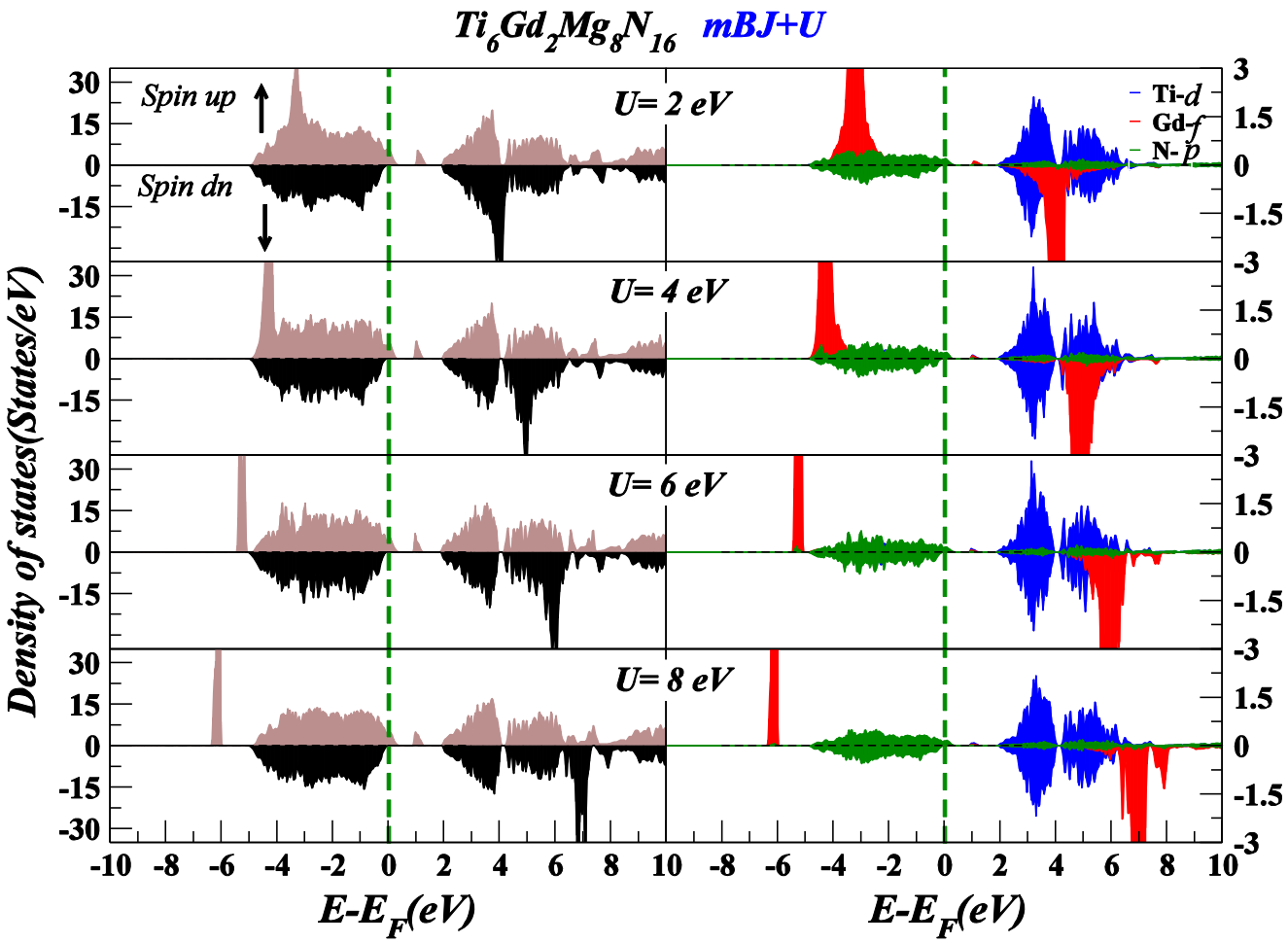

Fig. 8 Total and partial densities of states of the ferromagnetic $Ti_6Gd_2Mg_8N_{16}$ system using TB-mBJ + U approach (U varies from 2 eV to 8 eV)

correlation between the 4*f* electrons in Gd ion. First, the atomic internal positions were relaxed using the MINI package of the WIEN2k code. Table 1 shows total energies before and after the relaxation as function of the Hubbard potential.

From Figs. 5 and 6, GGA + *U* calculations show that the total energy of the ferromagnetic ordering for the near configuration is lower and should be the most appropriate to the spin arrangement of Gd than for all others phases.

In this section, we investigated the electronic properties of the doped system using GGA + *U* and TB-mBJ + *U* approximations. Figures 7–8 show the calculated total and partial densities of states of the ferromagnetic $Ti_6Gd_2Mg_8N_{16}$ material for different U values. In each figure, the upper panel shows the DOS of majority (↑) spin channel, and the lower panel is for the minority (↓) spin states. The Fermi level is at zero energy (green line).

GGA + *U* calculations predict a metallic character for the doped alloy in both spin directions (see Fig. 7). The partial densities of states indicate that the U value in GGA + *U* formalism has no significant effect on N-2*p* states in the valence band. Near the Fermi level E_F, Gd-4*f* states of the conduction band move away from Ti-3d orbitals to higher energies with the increase of U value.

The correct band gaps of semiconductors are highly desirable for their effective use in optoelectronic and other photonic devices. However, the theoretical results of the exact band

Table 2 The gap energy for minority spin and the calculated local and total magnetic moments in the FM phase using TB-mBJ + *U* approach

	E_g (minority spin) eV	Tot (μ_B)	Gd (μ_B)
U = 2 eV	1.859	12	6.762
U = 4 eV	1.868	12	6.820
U = 6 eV	1.878	12	6.855
U = 8 eV	1.910	12	6.881

Table 3 Curie temperatures and energy difference ΔE between AFM and FM arrangements of Gd spins as function of the effective Coulomb interaction

U (eV)	ΔE (meV)	T_C (K)
2	77.519	599.713
4	61.332	474.487
6	75.804	586.448
8	222.48	1721.179

gaps are quite challenging to reproduce. These semiconductors have a mixed binding character, where several electrons reside in the intestinal regions, which are difficult for proper theoretical treatment. For this, comparison of the calculated band gaps by different approximations shows that none of these methods is effective in reproducing the precise experimental band gaps of semiconductors.

To better analyze the Fermi region of densities of states of our doped system, the band gaps are re-examined and successfully reproduced by properly treating the density of electrons using TB-mBJ + *U* approach (Fig. 8) in order to make a detailed comparison of the obtained results by the two approximations. As shown in Fig. 8, the majority spin channel presents a metallic character, whereas in the minority spin channel, an energy gap exists around the Fermi level. We have summarized our results in Table 2. We see that the band gap increases from 1.856 eV to 1.910 eV for U = 2 eV and U = 8 eV, respectively, which depicted that $Ti_6Gd_2Mg_8N_{16}$ is half-metallic for all Hubbard parameter used (see Table 2).

As it is known, half-metallic ferromagnets are seen as a key ingredient in future high-performance spintronic devices, because they have only one electronic spin channel at the Fermi energy and, therefore, may show nearly 100 % spin polarization.

From all these findings, we believe strongly that the TB-mBJ + *U* functional is a very useful development for treating the electronic structure of our semiconductor alloy.

The electronic structure calculation reveals that it is half-metallic ferromagnet with the half-metallic gap of the order of 1.910 eV for U = 8 eV. Compatible with some important semiconductors, like $Cr_xZn_{1-x}Te$ [24], $T_{1-x}Cu_xMnSb$ (T = Ni, Co) [25], CdS:Eu [26], and many examples, our half-metallic material could be useful in spintronics.

The calculated total and local magnetic moments per atom of Gd-doped $Ti_{0.5}Mg_{0.5}N$ alloy are summarized in Table 2. TB-mBJ + *U* results show that the total magnetic moment contribution comes mainly from the Gd ions. The calculated total magnetic moment is 12 μ_B for all values of U, and it is exactly an integer value as expected for the half-metallic compounds [27]. From Table 2, it can be seen that the magnetic moment of Gd atom increases with the increase of the Hubbard value.

All theoretical approach based on the density functional theory (DFT) underestimates largely the band gap comparing to the experiment. On the other hand, the magnetic moment of Gd atom is equal to 7 μ_B, and TB-mBJ + *U* results show that the magnetic moment increases by varying the U-potential from 2 eV (6.762 μ_B) to 8 eV (6.881 $\mu_B \sim 7\ \mu_B$).

The absence in the literature of any experimental or theoretical information about the electronic structure and magnetic properties of this compound has led us to use the band gap and the magnetic moment of Gd atom as two basic criteria to select the better U. We can deduce that the value of 8 eV is more appropriate to this kind of material.

In order to estimate the curie temperature T_C of our studied system, we have used the Heisenberg model [28]:

$$U = -2J_{ij}\overrightarrow{S}_i\overrightarrow{S_j} \tag{3}$$

where S_i and S_j are the electron spins of Gd at site i and j and J_{ij} is the exchange integral between sites i and j. We can establish a relation between the exchange integral J and temperature T_C if we use the total energy difference $\Delta E = E_{AFM}–E_{FM}$ in this model within the mean field approximation as:

$$\Delta E = 2S(2S+1)J \tag{4}$$

And by using the Brillouin function expression, we obtain:

$$K_B.T_C = \frac{2}{3}\Delta E \tag{5}$$

where K_B is the Boltzmann constant. With this way, we can evaluate T_C from first-principles calculations, which are summarized in Table 3. It can be seen that T_C increase with the increase of U since the total energy is also affected by this parameter.

4 Conclusions

In this paper, we have studied the magnetic phase stability and electronic properties of Gd-doped $Ti_{0.5}Mg_{0.5}N$ alloy using L/APW + lo method. We have found that our doped alloy depicted a ferromagnetic character and TB-mBJ + *U* calculations of the DOS show that it is a half-metallic (HM) ferromagnet. We also estimated the Curie temperature average of about 350 k using the Heisenberg model in the mean field approximation.

As a whole, this leads us to conclude that Gd-doped $Ti_{0.5}Mg_{0.5}N$ alloy can be a potential candidate for promising spintronic applications, and we strongly solicit the experiment to verify these findings.

References

1. De Groot, R., Mueller, F., Van Engen, P., Buschow, K.: Phys Rev Lett. **50**, 2024 (1983)
2. Fang, C.M., De Wijs, G., De Groot, R.: J Appl Phys. **91**, 8340 (2002)
3. Kaminska, M., Twardowski, A., Wasik, D.: J Mater Sci Mater Electron. **19**, 828 (2008)
4. C. Fong, J. Pask, and L. Yang, Half-metallic materials and their properties, Vol. 2 (World Scientific, 2013).
5. Özdogan, K., Galanakis, I., Sasioglu, E., Aktas, B.: J Phys Condens Matter. **18**, 2905 (2006)
6. Xu, Y.-Q., Liu, B.-G., Pettifor, D.: Phys Rev B. **66**, 184435 (2002)

7. Sanyal, B., Bergqvist, L., Eriksson, O.: Phys Rev B. **68**, 054417 (2003)
8. Schwarz, K.: Journal of Physics F: Metal Physics. **16**, L211 (1986)
9. Coey, J., Chien, C.: MRS Bull. **28**, 720 (2003)
10. Swagten, H.: The magnetic behavior of diluted magnetic semiconductors. Springer, Boston (1990)
11. Zenasni, H., Faraoun, H., Esling, C.: J Magn Magn Mater. **333**, 162 (2013)
12. Alling, B.: Phys Rev B. **89**, 085112 (2014)
13. van de Walle, A., Tiwary, P., de Jong, M.M., Olmsted, D.L., Asta, M.D., Dick, A., Shin, D., Wang, Y., Chen, L.-Q., Liu, Z.-K.: Calphad. **42**, 13 (2013)
14. Zunger, A., Wei, S.H., Ferreira, L.G., Bernard, J.E.: Phys Rev Lett. **65**, 353 (1990)
15. Hohenberg, P.P.H., Kohn, W.: Phys Rev Lett. **136**, B864 (1964)
16. Kohn, W., Sham, L.J.: Phys Rev Lett. **140**, A1133 (1965)
17. Blaha, P., Schwarz, K., Madsen, G.K.H., Kvasnicka, D., Luitz, J.: WIEN2K, An augmented plane wave plus local orbitals program for calculating crystal properties. Vienna University of Technology, Vienna (2001)
18. Sjöstedt, E., Nordstrom, L., Singh, D.J.: Solid State Commun. **114**, 15 (2000)
19. Perdew, J.P., Burke, K., Ernzerhof, M.: Phys Rev Lett. **77**, 3865 (1996)
20. Tran, F., Blaha, P.: Phys Rev Lett. **102**, 226401 (2009)
21. Anisimov, V.I., Zaanen, J., Andersen, O.K.: Phys Rev B. **44**, 943 (1991)
22. Murnaghan, F.D.: Proc Natl Acad Sci U S A. **30**, 5390 (1944)
23. Wang, B., Gall, D.: Published in the proceedings of the 2018 IEEE Nanotechnology Symposium (ANTS), pp. 1–5. Albany, NY (2018)
24. Liu, Y., Liu, B.-G.: J Phys D Appl Phys. **40**, 6791–6796 (2007)
25. Galanakis, I., Şaşıoğlu, E., Özdoğan, K.: Phys Rev B. **77**, 214417 (2008)
26. Zhao, R., Pan, W., Yang, T., Li, Z., Xiao, B., Zhang, M.: J Phys Chem C. **51**, 28679–28684 (2015)
27. Pickett, W.E., Moodera, J.S.: Phys Today. **54**, 39 (2001)
28. Shi, S.Q., Ouyang, C.Y., Fang, Q., Shen, J.Q., Tang, W.H., Li, C.R.: EPL. **83**, 69001 (2008)

Publisher's note Springer Nature remains neutral with regard to jurisdictional claims in published maps and institutional affiliations.